Joint 20th AIRAPT – 43th EHPRG, June 27 – July 1, Karlsruhe/Germany 2005

A failure wave phenomenon in brittle materials

G.I. Kanel, S.V. Razorenov, V.E. Fortov
Institute for High Energy Densities of Russian Academy of Sciences
email: kanel@ficp.ac.ru

The failure wave is a network of cracks that are nucleated on the surface and propagate into the stressed body. In the paper, main results of observations of the failure wave phenomena are briefly reviewed and summarized. The discussion includes general behavior of glasses under shock compression, the conditions of initiating the failure waves, the failure wave speed and kinematics, state of glass behind the failure wave, and shock response of glass piles.

1. Introduction

The impact loading of a glass and, probably, other brittle materials can result in the appearance of a failure wave. The failure waves present a mode of catastrophic fracture in elastically compressed media that is not limited to impact events. One may hope that the investigations of failure waves provide information about the mechanisms and general rules of nucleation, growth, and interaction of the multiple cracks under compression.

The term “failure wave” has been introduced by Galin and Cherepanov, 1966, who developed a detonation-like model of fracture of stressed brittle materials. A stimulus for developing this theory was observation by Galin et al., 1966, who reported an explosion-like fracture under bending of high-strength glass from which the surface defects had been removed. The explosive fracture resulted in formation of micrometer-size glass particles. Basing on these experiments, a hypothesis has been suggested that supposes an ability of fragmentation occurring within relatively thin layer which propagates through undamaged material with the sound speed. Within this self-propagating layer, the potential energy of stressed body is transformed into a surface and kinetic energy of its fragments. Corresponding bibliography and critical analysis of different ways of describing the assuming failure waves can be found in the papers by Grigoryan, 1977, and Slepyan, 1977. One has to say the first models did not provide a base for correct estimations of the propagation velocity and other kinematical parameters of the failure waves. In particular, it was supposed the failure wave speed is equal to the sound speed or even exceeds this value that was not confirmed by any measurements.

A similar fracture mode under compression was revealed in shock-wave experiments as a response to planar shock-wave compression of glasses below the Hugoniot elastic limit. The history and some preliminary results of observations of the failure wave phenomena were reviewed by Brar, 2000, Kanel and Bless, 2002, and Kanel, Razorenov and Fortov, 2004. In this paper we are concentrated on main properties of the failure waves.

2. The method

In the experiments, one-dimensional shock loads were created in the samples by impacts of flyer plates launched with explosive facilities or with a gas gun. Using plane impactors of different thickness the shock load duration was varied whereas the impact velocity controlled the peak shock stress (see Antoun et al, 2003). The dynamic yielding and the spall fracture appear in the structure of compression and rarefaction waves which is recorded by monitoring the free surface velocity histories with the VISAR laser Doppler velocimeter (Barker and Hollenbach, 1974).

3. Behavior of glasses under shock compression

Silicate glasses exhibit a high yield strength and low fracture toughness as a result of their high homogeneity. The fracture of glasses under compression occurs by axial splitting. At high pressures, brittle glasses become ductile. Ductility of glass is caused by a loose microstructure with a large concentration of molecular-size voids. It is known that glasses show gradual structural changes resulting in increased density (Arndt and Stöffer, 1969). Since densification occurs under Vickers indentation, it is supposed (Ernsberger, 1968) that the irreversible densification of the silicate structure is responsible for the plastic flow properties of glasses under high pressure. The degree of densification can be varied to some extent by variation of pressure, temperature, and shear strain, and remains irreversible under normal conditions. Irreversible densification of some glasses also occurs under shock compression above the HEL (Gibbons and Ahrens, 1971).

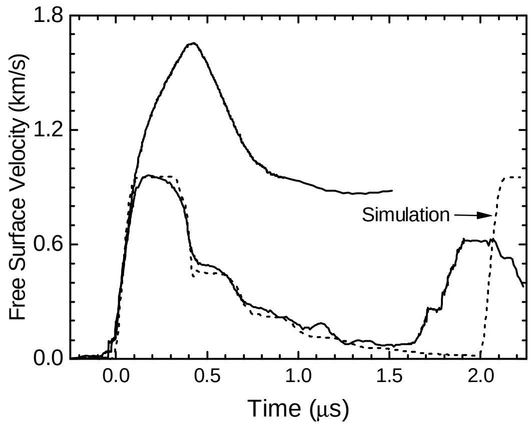

Fig. 1. Experimental results for 6.1-mm-thick K8 crown glass samples impacted at 670 ± 30 m/s by a 0.9-mm-thick steel flyer plate and at 1900 ± 50 m/s by a 2-mm-thick aluminum flyer plate backed by paraffin. The dashed line shows results of computer simulations assuming no failure to occur.

Figure 1 presents free surface velocity profiles for K8 crown glass which were measured at two different impact velocities (Kanel et al., 1998). The collision of flyer plate with the plane sample creates uniaxial compression wave which propagates from the impact surface toward the rear surface of the sample and causes acceleration of the latter. The initial sequence of the velocity history, which reproduces the stress profile of the compression pulse inside the plate, exhibits all main peculiarities of the response of glasses. The free surface velocity histories do not exhibit a distinct transition from the elastic to plastic response. The compression wave in glass exhibits a gradual increase of rise time with the increase of the propagation distance as a result of its anomalous compressibility. Above the elastic limit a long rise time of the compression wave is due to a rate-dependent inelastic deformation.

The compression wave is followed by unloading. Duration of the compression pulse is controlled by the time of wave reverberation in the impactor plate. When a compression pulse reaches the body surface, a reflected tensile wave is generated. As a result of the tension in the reflected wave, the so called spall fracture may occur. Spallation was not observed in these shots, which means that the spall strength of the glass exceeds 6.8 GPa below the HEL and remains very high above the HEL. For comparison, the static tensile strength of glasses is around 0.1 GPa. The reason for such a large discrepancy is that the fracture nucleation sites in homogeneous glass are concentrated on the surface. These incipient microcracks are activated and determine the strength magnitude in the static measurements, whereas spall strength is an intrinsic property of matter.

In Fig. 2 the free surface velocity histories of several different glass samples are shown. It is known that silicate glasses have anomalous compressibility within the elastic deformation region. Most of silicate glasses have anomalous longitudinal compressibility within the region of elastic compression where the longitudinal sound speed decreases as the compressive stress increases that, in turn, causes broadening of the elastic compression wave with its propagation. It is not clear yet whether or not the bulk compressibility of glasses is anomalous also. As a result of an anomalous decrease of longitudinal sound speed with increasing stress, a rarefaction shock wave should be formed in glass at unloading from a shock-compressed state. Obviously, this may occur only in the case that the compression is completely reversible. Since the reversibility of stress–strain processes is a main attribute of

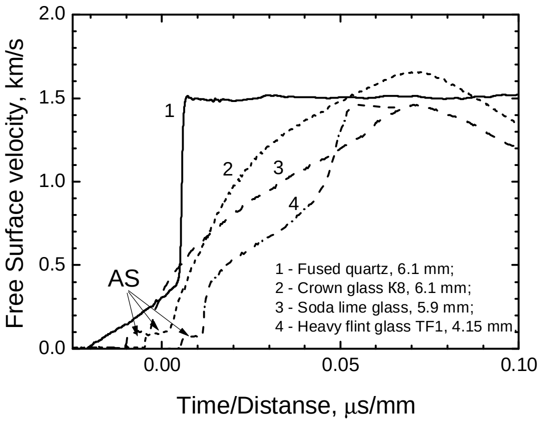

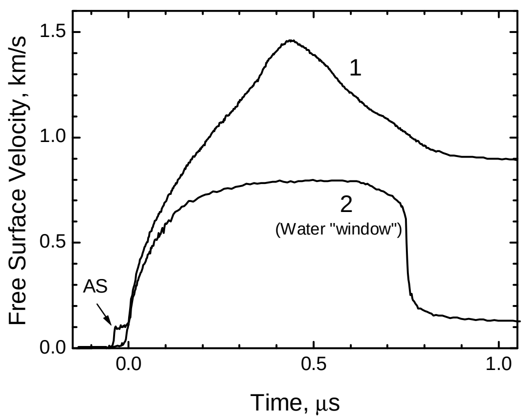

Fig. 2. Structure of the compression waves in fused quartz (Kanel, Bogach, et al., 2004), K8 crown glass (Kanel et al., 1998), soda lime glass (Kanel, Bogach, et al., 2002) and TF1 heavy flint glass (Kanel, Bogach, et al., 2004). The weak velocity steps AS before the main front is obviously the result of an air shock propagating ahead of the flyer plate.

Fig. 3. Free surface velocity histories of soda lime glass plates of thickness 5.9 mm (Kanel, Bogach, et al., 2002). The wave profile 1 corresponds to impact by aluminum flyer plate of 2 mm thick backed by paraffin, with the impact velocity being 1.90±0.05 km/s. The wave profile 2 corresponds to impact by aluminum flyer plate of 2.1 mm thick at the impact velocity 0.97±0.03 km/s, measured through a water window.

elastic deformations, observation of the rarefaction shock (demonstrated by the waveform 2 in Fig. 3) may be considered as evidence of an elastic regime of deformation. Above the Hugoniot elastic limit (HEL) the unloading wave speed becomes greater than the compression wave speed that is demonstrated by the waveform 1 in Fig. 3.

4. Observations of the failure waves

4.1. Cracking of glass near the impact surface

In the Fig. 1 the results of the measurements are compared with the computer simulation for the shot of K8 glass target impacted by a low-velocity steel plate. Simulation has been done supposing purely elastic behavior for the glass, and without fracture under both compression and tension. It can be seen that the computed first velocity pulse is in a reasonable agreement with the measured one. This agreement confirms the mainly elastic response of the glass in this stress range. A step-like velocity decreasing in the unloading is a result of disagreement in dynamic impedances between the glass target and the steel impactor. Compared to the simulation, in the experiment the second velocity pulse arrives at the rear surface earlier. Also, it has less steep slopes in both compression and unloading and less magnitude than the calculated one. These differences mean that the observed second velocity pulse is actually a reflection of the rarefaction wave from a near-surface layer which is not able to sustain tension. In other words, the layer of glass near the impact surface has been failed to the moment when the reflected tensile pulse reached it. Expansion of the cracked layer from the impact surface has been treated as propagation of the failure wave. As a result of cracking, a glass looses its optical uniformity that gives a possibility of optical recording these processes. Using this circumstance, Bourne et al., 1995, and Senf et al., 1995, have photographed failure waves in transmitted light.

4.2. Initiating conditions of the failure waves

Raiser et al., 1994, have found that a surface roughness of aluminosilicate glass between 0.04 and 0.52 μm does not appear to play a significant role in the formation of a failure wave.

Independently of the surface roughness, they observed a high spall strength of the glass when the compressive stress was around 3.5 GPa whereas, at peak stresses of 7.5–8.4 GPa, the spall strength was high ahead of the failure front and was low behind it. Bourne et al., 1997, have found that deliberately introducing flaws by roughening the surface speeds the fracture of a glass, increasing the average failure-wave velocity. Kanel et al., 2002, have found that, although the failure waves are formed in glass independently on the roughness of its surface, the shock-wave behavior of lapped glass plates is much more reproducible than that of as-received plates with mirror-like surfaces.

4.3. The failure wave speed

Whether the failure wave is steady or it decays and stops at some distance is an important issue for understanding the mechanism and nature of the phenomenon. A series of shock-wave experiments with soda lime glass plates of different thicknesses have been performed in order to evaluate the failure wave speed at various stress levels and propagation distances. The measured free surface velocity histories are presented in Fig. 4 where the time is normalized by the sample plate thickness.

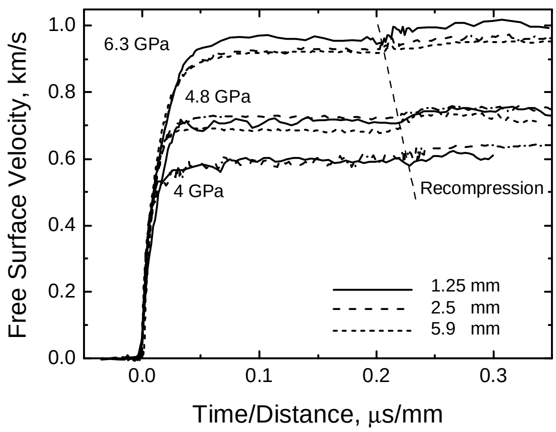

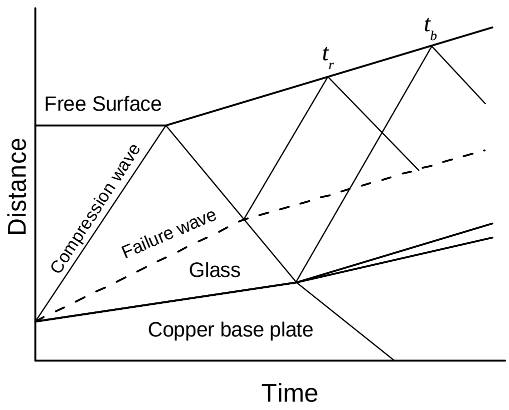

Fig. 4. Free surface velocity histories of the soda lime glass plates of different thicknesses at three different stress levels of shock compression.

Fig. 5. Distance-time diagram of experiments shown in Fig. 4.

The wave profiles contain small recompression pulses which are due to the wave reflection from a failed region inside the sample (see Razorenov et al., 1991, Brar and Bless, 1992, Dandekar and Beaulieu, 1995). It follows from consideration of the time–distance diagram shown in Fig. 5 that the failure wave speed c_f is determined by means of measurement of the time interval t_r between the arrivals of the initial compression wave and the recompression pulse front at the plate free surface, with the following relationship

$$c_f = \frac{x}{t_x} = c_l \frac{2 - c_l t_r / \delta}{2 + c_l t_r / \delta} \qquad (1)$$

where x is the location of the failure wave front at time t_x, and δ is the glass plate thickness. It follows from Eq. (1) that for constant speed of the failure wave the ratio t_r/δ should not depend on the plate thickness.

As shown in Fig. 4, the failure waves indeed propagate at a constant speed which depends only on the stress level. Using the average value of 5.3 km/s for the sound speed we could find that the failure wave speed decreases from 1.58±0.06 km/s at the compressive stress of 6.3 GPa ahead of the failure front to 1.35±0.06 km/s at the compressive stress of 4 GPa. The observed constant speed of the failure wave is in agreement with the data by Dandekar and Beaulieu, 1995. The stress dependence of the failure wave speed explains its apparent deceleration that was found in the first observation by Razorenov et al., 1991, where the glass samples were loaded by decaying stress pulses. The failure wave process becomes unstable, and stops at the stress level near the failure threshold. Comparison of the time t_r of arrival of re-reflected pulses in Figures 1 and 4 shows that the reflected signal arrives later in the case of short loading pulse. The latter observation indicates that unloading from the impactor decreases the failure wave velocity or even arrests the failure wave propagation.

4.4. State of glass behind the failure wave

Brar et al., 1991, 1992, Bless, et al., 1992, and Bourne et al., 1996, have shown by direct measurements on different glasses that behind the failure wave the tensile strength drops to zero, or almost to zero, and the transverse stress increases, indicating a decrease in shear strength. Figure 6 summarizes the results of stress difference measurements by Brar et al., 1991a, and Kanel et al., 1977.

The failure waves were recorded in the longitudinal stress range 4–10 GPa; for this stress range the diagram shows the stress difference ahead of, and behind, the failure front. It looks quite reasonable that reduction of the final stress difference with an increase of the shock amplitude, and, respectively, an increased degree of comminution occurs. At peak stresses exceeding 10 GPa, the densification processes start in glass. This produces shear stress relaxation without cracking. A second rise in the stress difference at ~15 GPa may be evidence that maximum densification has been achieved.

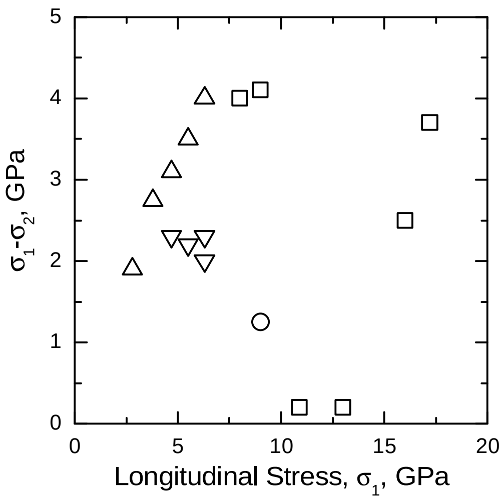

Fig. 6. Results of measurements by Brar et al., 1991 (triangles) and Kanel et al., 1977 (squares and circles) of the stress difference in shock compressed glass as a function of the peak stress.

4.5. Kinematics of the failure waves

Since the first experimental observations of failure waves in shock-compressed glass it was believed that the failure wave is accompanied by increasing lateral stresses and is not accompanied by any change in longitudinal stresses. However, recent experiments of Dandekar, 1998, and of Millet et al., 1998, revealed a disagreement between the longitudinal stress measured on the impact surface of a shock-loaded glass plate and the stress measured at some distance from the impact surface. Although the recorded wave profiles had a rectangular shape without any signature of a second compression wave, the measured stresses at some distance were less than at the impact surface when the incident shock amplitude exceeded some threshold. These observations may be treated as evidence of formation of an unrecorded second compression wave, and perhaps this should be identified as the failure wave. The kinematics of failure wave phenomena were investigated in more detail by Kanel et al., 2002.

Figure 7 presents stress histories measured by Kanel et al., 2002, on input and output surfaces of glass samples. Measurements confirm the difference between peak stresses measured on the impact surface of a shock-loaded glass plate and the stresses measured at some distance from the impact surface, as observed by Dandekar and by Millet et al. The stress measured by the first gauge in Fig. 7 is 6.6 GPa, whereas the second gauge recorded a 6.1 GPa stress between two glass plates at a distance of 5.85 mm from the input surface of the glass sample. Similar experiments by Kanel et al., 2002, with layered glass samples have shown that the network of growing microcracks in shock-compressed glass may indeed be considered as a wave with a small stress increment which obeys the Rankine-Hugoniot conservation laws.

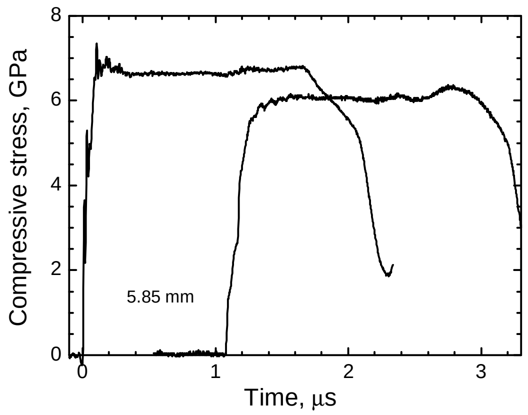

Fig. 7. Stress histories on the input and output surfaces of glass sample. Graph represents the experimental result with a thick glass plate backed by another glass plate of the same thickness.

Thus, we come to the conclusion that, when a failure wave is formed, shock compression of glass leads to a two-wave structure. The failure wave is really a wave process, but its kinematics differ from those of elastic−plastic waves. The shock compression wave in an elastic−plastic body becomes unstable as a result of the sudden decrease of longitudinal compressibility that occurs when yielding begins. As a result, the wave splits into an elastic precursor wave and a plastic shock wave. The peak stress behind the elastic precursor front is the HEL, which is determined by the yield stress. A similar wave structure should be seen in a polycrystalline brittle solid where the HEL corresponds to the failure threshold stress and fracture occurs locally in each grain (or around grains) immediately when an applied stress exceeds the failure threshold. Note that, in both these cases, the propagation velocities of the elastic precursor wave front and the second compression wave are determined by the longitudinal and bulk compressibility, respectively.

However, the propagation velocity of the failure wave is determined by the crack growth speed, which is not directly related to the compressibility. On the other hand, the final longitudinal stress in the comminuted glass behind the failure wave is determined by the impact conditions, whereas the deviator stress component is controlled by the post-failure material properties. Thus, since the propagation velocity of a failure wave and the final stress are fixed, the stress in the leading elastic wave should be governed by these values and should not necessarily be equal to the failure threshold. The glass surface plays an important role in the failure-wave process because the surface is a source of cracks. In this sense the process is similar to diffusion. When the stressed state is maintained, the subsonic failure wave may evidently propagate in a self-supported mode like a combustion wave.

Figure 8 presents the stress−strain diagram of shock compression of soda lime glass. The slope of the $\sigma_x(\varepsilon_x)$ curve decreases with increasing stress as a result of anomalous compressibility of the glass. The bulk compressibility of glass is assumed to be constant: $p = -\rho_0 c_b^2 (\Delta V/V_0)$, where c_b = 4.24 km/s is the bulk sound speed at zero pressure and V is the specific volume. The estimated final state is above the pressure curve by the amount $\sigma_x - p$ = 1.4 GPa. Since the hydrostatic pressure is the average stress

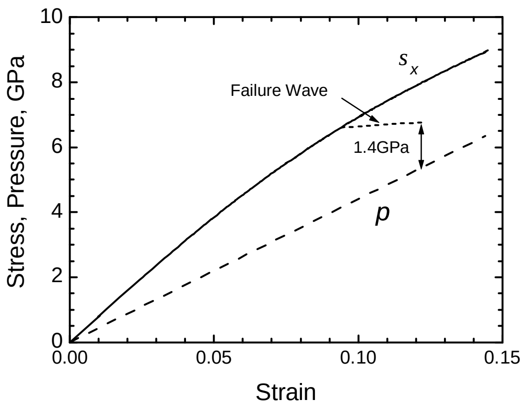

Fig. 8. The stress−strain diagram of glass under shock compression. The dashed line shows the assumed linear bulk compressibility, and short-dashed line illustrates the failure wave process.

$p = (\sigma_x + 2\sigma_y)/3$, we may estimate the principal stress difference to be $\sigma_x - \sigma_y = 3(\sigma_x - p)/2 = 2.1$ GPa. Brar et al., 1991, carried out direct measurements of the principal stress difference and got 2.0−2.3 GPa behind the failure wave in soda lime glass (see Fig. 6).

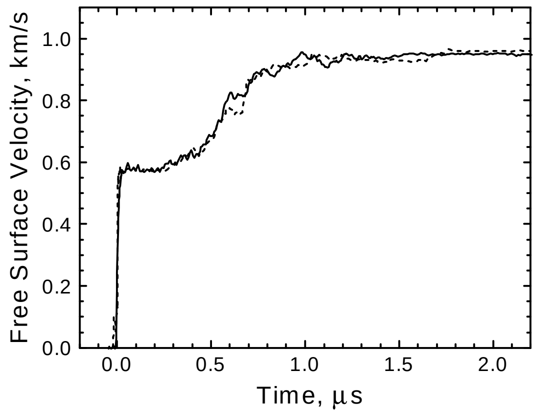

Fig. 9. The free surface velocity histories recorded in two shots with layered assemblies of 8 soda lime glass plates of 1.21 mm average thickness. Data by Kanel et al., 2002.

4.7. Shock response of glass piles

Since the failure wave nucleates on the glass surface, the magnitude of the leading elastic wave in the shocked specimen consisting of layered glass plates should decrease as a result of its decomposition into two waves at each interface. The decrease of elastic wave amplitude repeats at each interface until the failure threshold is reached. Hence, for a sufficiently large number of layered glass plates, an elastic precursor wave with its amplitude close to the failure threshold could be formed. Figure 9 presents results of two shots where free surface velocity histories were recorded for layered assemblies of 8 glass plates of average thickness 1.21 mm, subjected to the same impact loading. The results with good reproducibility show the waveform that is typical for elastic−plastic solids. The magnitude of the elastic precursor wave is 4.0 GPa. The final free surface velocity is practically equal to that of a single glass plate.

The response of a layered assembly of thin brittle plates as compared to that of one thick plate is a simple way to diagnose nucleation of the failure process on the plate surfaces and determine the failure threshold. As an illustration, Figs. 10 and 11 show the results of such experiments with fused quartz and K8 crown glass. The failure wave phenomenon is obviously a common one for different glasses but the threshold stress differs depending on the glass properties.

4.8. Failure waves at peak stresses above the Hugoniot elastic limit.

Figure 12 demonstrates the free surface velocity history with the assembly of 5 soda lime glass plates of 1.2 mm in thickness impacted by an aluminum flyer plate at the velocity of 1.9 km/s, in comparison with the results for single glass plates at the same and lower peak

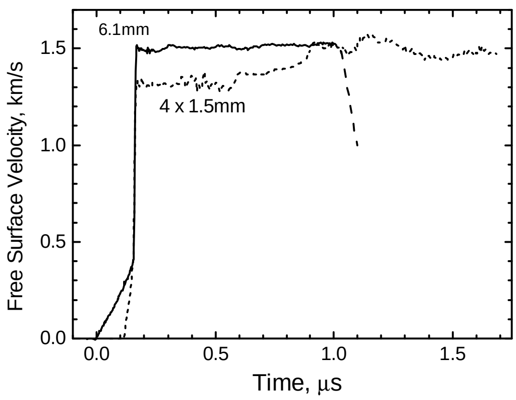

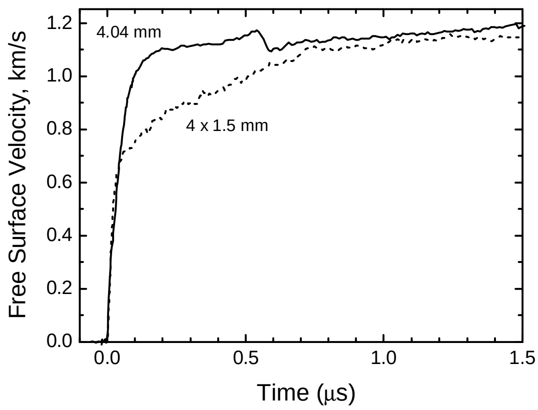

Fig. 10. The free surface velocity histories of one thick plate and a layered assembly of four thin plates of fused quartz under the same impact conditions.

Fig. 11. The free surface velocity histories of one thick plate and a layered assembly of four thin plates of K8 crown glass under the same impact conditions.

stresses. The shock pulse obviously decayed to approximately 9.5 GPa near the sample rear surface because of the relatively small thickness of the flyer plate (2 mm). With the same total sample thickness and the same peak stress, the total rise time is less for the glass plate assembly than that for a single glass plate. A reason of this discrepancy is partially due to the thin gaps between thin glass plates. The total time of propagation of the wave front through the assembly is the sum of the individual time of wave propagation through each plate and the time of closing these gaps. Since the wave speed is much higher than the speed of closing the gaps, even a very thin gap markedly reduces the average propagation velocity of the wave front. The gaps become closed ahead of the upper part of compressive wave so the velocity of the latter in the assembly is the same as that in a single plate.

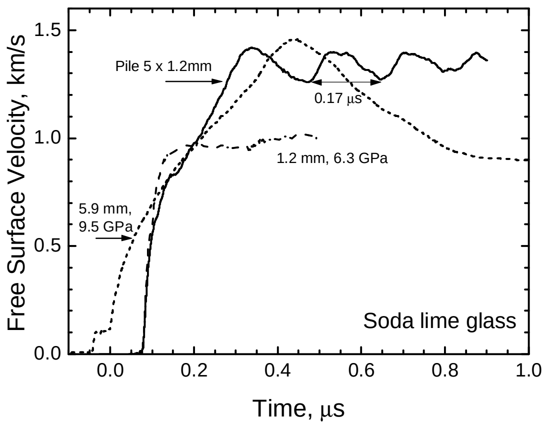

Fig. 12. The free surface velocity history with the assembly of 5 soda lime glass plates of 1.2 mm in thickness impacted by an aluminum flyer plate of 2 mm in thickness at 1.9±0.05 km/s impact velocity, in comparison with the results for single plates at the same and lower peak stresses. A weak velocity step before the main front in the free surface velocity history of a single glass plate of 5.9 mm thick is due to an air shock in front of the flyer plate.

The waveform for the glass plate assembly demonstrates a steeper plastic part than that for the single plate. As it could be expected, the velocity "pullback" in the unloading part of the stress pulse is less for the assembly than that for the single plate because the assembly can not sustain tension at the interfaces between plates. The velocity oscillations in the residual part of the waveform are the result of wave reverberations inside the last plate of the assembly. The period of these oscillations is about 0.17 µs whereas its expected value for undamaged plate is $\Delta t_{exp} = 2d_{lp}/c_{l} = 0.42$ µs (where d_{lp} is the thickness of last plate). We may conclude that a part of the last glass plate in the assembly has been damaged by the failure wave. In this case, a steeper plastic part of the waveform implies that the comminuted glass has less viscosity than undamaged material. On the other hand, the reverberation time of 0.17 µs in the shot at the peak stress of 9.5 GPa is less than 0.25 µs of the time when the recompression signal appears in the free surface velocity history at the 6.3 GPa peak stress. We may assume a higher velocity and longer propagation time of the failure waves in the shot at high stress.

It has been claimed earlier that the failure wave phenomena occur when the impact stress exceeds the failure threshold but is still below the HEL of a glass, and that the ductility hinders the microcracking in the glass. The experimental result presented in Fig. 12 for single glass plate also do not reveal any evidence of fracture and the failure wave process in this stress range. Under gradual compression with a smoothed wave of enough high peak stress, however, the microcracking may occur within a short time interval between the time when the failure threshold is reached and the time when the plastic yielding begins. In the experiments, the consequence of compressive fracture evinces itself in shortening the wave reverberation time in the glass plate assemblies.

As a result of anomalous compressibility and the elastic-plastic transition, the compressive discontinuity at impact loading is transformed to a rather ramped compressive wave. Accounting for this circumstance, Figure 13 illustrates the propagation of a compressive wave and the failure waves through a glass plate assembly. The total rise time of the compressive wave increases with the distance. The failure waves are nucleated at each plate surface in the assembly when the failure threshold is reached, and are stopped when they meet the part of compressive wave where plastic yielding occurs. Due to the expanding of compression wave, the time and distance of propagation of the failure waves are the smallest for the first plate in the assembly but they increase as the compressive wave propagates through the assembly. In other words, contribution of the failure wave phenomenon is negligible near the impact surface, and increases with the propagation of the compressive wave through the assembly. On the other hand, the smaller propagation distance of the failure wave results in its smaller influence on the waveform at shock compression above the HEL.

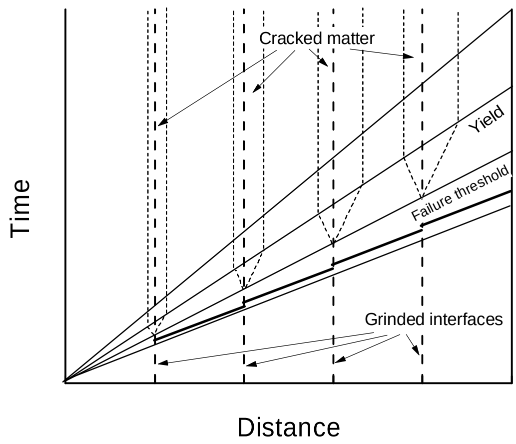

Fig. 13. Assumed time–distance diagram of the failure wave phenomena in a glass plate assembly impacted above the HEL.

The failure waves moving in the impact direction meet the yielding threshold after a longer time of propagation than that for the failure waves moving in the opposite direction. This produces the asymmetry in the distribution of microcracking with respect to the interfaces between plates.

In this regard, it is interesting to mention the peculiarity of localized inelastic deformation following the shock compression of K8 crown glass above the HEL as observed by Kanel and Molodets, 1976. In this study, the distortion of internal interfaces of the two-piece glass targets resulted in the elongation of the manganin piezoresistive foil gauges used for recording the stress profiles. Figure 14 demonstrates both the stress history and the component of gauge resistance increase due to its elongation. The gauges were placed in a gap between glass plates together with insulating Teflon films. The films had different thicknesses so that the gauges positions were asymmetrical with respect to the middle sections of the gaps. A microcrack leads to the distortion of the glass plate surface that in turn leads to the elongation of the gauge pressed to it. The foil gauges sense the surface distortion if the size of the non-uniformity is comparable to, or larger than, the thickness of the gauge foil. The distortion is higher in the gauge next to the receiving block that correlates with the asymmetry of the failure wave propagation between the failure threshold and the beginning of ductility as discussed above. The distortion was not recorded at the impact surface, and increased with the distance from the impact surface.

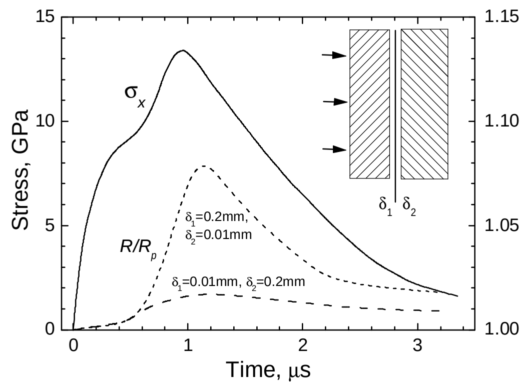

Fig. 14. Stress history and distortion of plate surfaces following the shock compression of K8 crown glass. Measurements were carried out at a distance of 10 mm from the impact surface with manganin and constantan gauges insulated by Teflon. Dashed lines show the component of the gauge resistance increase due to the elongation.

5. Discussions

The impact loading of a glass and, probably, other brittle materials can be accompanied by an appearance of a failure wave. The failure wave is a network of cracks that are nucleated on the surface and propagate into the stressed body. It presents a mode of catastrophic fracture in an elastically stressed media that is not limited to impact events. It has been shown that the failure wave is really a wave process with a small stress increment, although its kinematics differs from that of elastic-plastic waves. The propagation velocity of the failure wave is less than the sound speed, it is not directly related to the compressibility but is determined by the crack growth speed. The propagation speed of the failure wave slightly depends on the stress above the failure threshold, and does not depend on the propagation distance. The glass surface plays an important role in the failure wave process because the surface is a source of cracks. Transformation of elastic compression wave followed by the failure wave in a thick glass plate into typical two-wave configuration in a pile of thin glass plates confirms the role of surfaces that distinguish the failure wave process and time-dependent inelastic compressive behavior of brittle materials. At peak stresses above the Hugoniot elastic limit, the failure wave process may occur at gradual compression as the stress grows above the failure threshold up to the stress at which plastic deformation begins.

Experiments with the assemblies of thin glass plates confirm the appearance of the failure wave in elastically compressed glasses, although the relationships between the HEL and the failure thresholds are different for different kinds of glasses. These experiments unambiguously demonstrate the role of surfaces as a microcracking source in the overall response of a glass target to shock compression, and present an effective tool to reveal and diagnose the failure wave process. The introduction of internal surfaces is a way to separate the failure wave process and time-dependent inelastic compressive behavior of brittle materials. No evidence of the failure wave has been revealed for shock-compressed states well above the HEL of glasses. At the peak stresses above the HEL, however, the failure wave process may occur under a gradual compression as the stress grows above the failure threshold up to the stress at which plastic deformation starts.

The mechanism of failure wave propagation under compression is not yet completely clear. Note that the compressive fracture of glasses under quasi-static conditions occurs by axial splitting (Bridgman, 1964). Since the failure wave speed reaches the ultimate speed of cracks in glasses, it is natural to conclude that the failure wave consists of cracks propagating in the direction of compression. Probably, some mechanism of self-supporting propagation of rapid cracks exists. However, even with self-propagating axial cracks it is difficult to understand the observed shear stress relaxation. Branching or transverse cracking must also take place in the failure wave.

References.

Antoun T., Seaman L., Curran D.R., Kanel G.I., Razorenov S.V., Utkin A.V., 2003. *Spall Fracture*. Springer, New York.

Arndt J. and Stoffer D., 1969. Anomalous changes in some properties of silica glass densified at very high pressures. *Phys. and Chem. of Glasses*, **10**(3), 117-134.

Barker L.M. and Hollenbach R.E., 1974, *J. Appl. Phys.*, **45**(11), 4872-4887.

Bless S.J., Brar N.S., Kanel G.I., and Rosenberg Z., 1992. Failure Waves in Glass. *J.Amer. Ceram. Soc.*, **75**(4), 1002-1004.

Bourne N. K., Millet J.C.F., and Rosenberg Z., 1997. On the origin of failure waves in glass. *J. Appl. Phys.* **81**(10), 6670−6674.

Bourne N.K., Rosenberg Z., Field J.E., 1995. High-speed photography of compressive failure waves in glasses. *J. Appl. Phys.* **78**, 3736-3739.

Bourne N. K., Rosenberg Z., and Millet J.C.F., 1996. The Plate Impact Response of Three Glasses. *Structures under Shock and Impact IV,* N. Jones et al., eds. Computational Mechanics Publications, Southampton, 553–562.

Brar, N.S., 2000. Failure waves in glass and ceramics under shock compression. In: Shock Compression of Condensed Matter – 1999, eds: M.D. Furnish et al., New York, American Institute of Physics, CP **505**, 601-606

Brar N.S. and Bless S.J., 1992. Failure Waves in Glass under Dynamic Compression. *High Press. Res.* **10,** 773–84.

Brar N.S., Bless S.J., and Rozenberg Z., 1991. Impact-induced failure waves in glass bars and plates, *Appl. Phys. Lett.* **59**(26), 3396–3398.

Bridgman P., 1964. *Studies in Large Plastic Flow and Fracture*, Harvard University Press, Cambridge, MA.

Dandekar D.P., 1998. Index of refraction and mechanical behavior of soda lime glass under shock and release wave propagation. *J. Appl. Phys.* **84**(12), 6614–6622.

Dandekar D.P. and Beaulieu P.A., 1995. Failure Wave under Shock Wave Compression in Soda Lime Glass. In: *Metallurgical and Material Applications of Shock-Wave and High-Strain-Rate Phenomena.* Edited by L. E. Murr, K. P. Staudhammer, and M. A. Meyers. Elsevier, Amsterdam, Netherlands, 211–218.

Ernsberger F.M., 1968. Role of densification in deformation of glasses under point loading. - *J. Amer. Ceram. Soc*., **51**(10), 545-547.

Galin L.A. and Cherepanov G.I., 1966. On self-supporting failure of a stressed brittle solid. *Dokl. AN SSSR*, **167**(3), 543-546 (In Russian).

Galin L.A., Ryabov V.A., Fedoseev, D.V. and Cherepanov G.I., 1966. On failure of a high-strength glass. *Dokl. AN SSSR*, **169**(5), 1034-1036 (In Russian).

Gibbons R.V. and Ahrens T.J., 1971. Shock metamorphism of silicate glasses. *J. Geophys. Res.*, **76**(23), 5489-5498.

Grigoryan S.S., 1977. *Mekhanika Tverdogo Tela*, no 1, 173-181 (In Russian).

Kanel G.I. and Bless S.J., 2002. Compressive fracture of brittle solids under shock-wave loading. In: Ceramic Armor Materials by Design (eds. J.W. McCauley, A. Crowson, W.A. Gooch, A.M. Rajendran, S.J. Bless, K. Logan, M. Normandia, and S. Wax), *Ceramics Transaction*, **134**, 197-216.

Kanel G.I., Bogatch A.A., Razorenov S.V., Zhen Chen, 2002. Transformation of shock compression pulses in glass due to the failure wave phenomena. *J. Appl. Phys.*, **92**(9), 5045-5052.

Kanel G.I., Bogach A.A., Razorenov S.V., Savinykh A.S., Chen Z., and Rajendran A., 2004. A Study of the Failure Wave Phenomenon in Brittle Materials. In: Shock Compression of Condensed Matter – 2003, Eds. M. D. Furnish et al., AIP CP **706**, pp. 739-742.

Kanel G.I. and Molodets A.M., 1976. Behavior of type K-8 glass under in dynamic compression and subsequent unloading. *Sov. Phys.–Tech. Phys.* **21**(2), 226–232.

Kanel G.I., Molodets A.M., and Dremin A.N., 1977. Investigations of features of deforming a glass in intense compression waves. *Comb. Expl. Shock Waves* **13**(6), 772–773.

Kanel G.I., Razorenov S.V., Fortov V.E., 2004. Shock-Wave Phenomena and the Properties of Condensed Matter. New York, Springer, 320 pp.

Kanel G.I., Razorenov S.V., Utkin A.V., Hongliang He, Fuqian Jing, and Xiaogang Jin, 1998. Influence of the load conditions on the failure wave in glasses. *High Pressure Research*, **16**, 27-44.

Millet J., Bourne N., and Rozenberg Z., 1998. Observations of the Hugoniot curves for glasses as measured by embedded stress gauges. *J. Appl. Phys*. **84**(2), 739–741.

Raiser G., Wise J.L., Clifton R.J., Grady D.E., and Cox D.E., 1994. Plate impact response of ceramics and glasses. *J. Appl. Phys*. **75**(8), 3862–3869.

Rasorenov S.V., Kanel G.I., Fortov V.E., Abasehov M.M., 1991. The fracture of glass under high-pressure impulsive loading. - *High Pressure Research*, **6**, 225-232

Senf H., Strausburger E., and Rothenhausler H., 1995. Visualization of fracture nucleation during impact in glass. In: *Metallurgical and Material Applications of Shock-Wave and High-Strain-Rate Phenomena* (eds. L.E. Murret al.) Elsevier, Amsterdam, 163–170.

Slepyan L.I., 1977, *Mekhanika Tverdogo Tela*, no 1, 181-186 (In Russian).